DESIGN CONSIDERATIONS FOR A CDZNTE DIGITAL MAMMOGRAPHY SYSTEM

JAMES G. MAINPRIZE, MARTIN J. YAFFE, TÜMAY TÜMER[1], SHI YIN[1] AND WILLIAM J. HAMILTON[2]
Imaging Research, Sunnybrook Health Science Centre, University of Toronto, Toronto, Canada
[1]*Nova R & D Inc., Riverside, California, U.S.A*
[2]*Santa Barbara Research Center, Goleta, California, U.S.A.*

1. Introduction

In an effort to improve the performance of x-ray detectors for digital mammography, we are investigating the design of new direct conversion detectors for application in a slot-scanned system. The narrow slot geometry provides a dose-efficient means of scatter rejection and it allows the use of small detector modules to produce a full area image. The slot-scanned technique relies on CCD technology, using time-delay integration (TDI) for signal acquisition.

There are several solid state materials that may be used for an x-ray detector. Unlike phosphor-coupled devices which are *indirect* x-ray detectors, these materials convert the energy absorbed from the x-ray beam directly to an electronic signal.

One material that has recently become of interest is $Cd_{1-x}Zn_xTe$ (CZT). It has several properties that make it potentially useful for digital mammography. It has a high density (5.8 g/cm^3) and a high effective atomic number which provides an excellent quantum interaction efficiency even for very thin detectors (98% at 20 keV for 400 μm thickness). This material has a high resistivity (10-100 GΩ·cm) which allows reasonably low dark currents to be maintained. It also has a high signal gain (approx. 4000 electron-hole pairs for a 20 keV photon[1]) which provides an excellent signal to noise ratio.

In designing a new x-ray detector, the goal is always to produce a device uses x-rays efficiently to provide the highest possible image quality. By careful modeling of signal and noise propagation, the image quality of the prototype detector can be predicted. Using reasonable estimates of the requirements for image quality for mammography and the limitations imposed by the properties of CZT and the TDI acquisition technique, a range of design parameters can be determined. Within this range of parameters, there may exist an optimum set that yields the best possible image quality.

In this paper we examine the design requirements for the detector and develop a model which can be used to predict various descriptions of image quality. Some initial optimization results will also be presented.

2. Design Requirements

A detector for a digital mammography system must satisfy several very demanding requirements in terms of image quality, which are related to the clinical imaging tasks. One important task is the visualization and characterization of soft tissue masses and architectural distortions. This influences the required contrast sensitivity which must be maintained over a wide dynamic range representing variations in x–ray transmission due to changes in the composition and the thickness of the breast. The exposure at the detector may range from 10 mR to 1000 mR across the image[2]. In order to have good low contrast sensitivity over this range (e.g. 1%), the dynamic range necessary may be as high as 5000 to 10 000 depending on the x-ray spectrum.

The detection and characterization of microcalcifications is also an important imaging task. This requires very high spatial resolution. Studies have shown that at least 100 μm is required for simple detection[3]. To characterize and classify the microcalcifications, a higher resolution may be required.

Different spectra are used for different breast thicknesses, generally increasing kVp to increase penetration for thicker breasts. There is also evidence that different spectral filters may be suited to different thicknesses or tissue composition[4]. Therefore, the x-ray detector should behave well over the entire possible spectral range (approximately 16 to 30 keV).

3. Detector Design

Present technology allows the fabrication of CZT photoconductor arrays of a reasonable area of from up to 6.25 cm^2[1]. Although this is far too small for a full-area detector, it is certainly feasible to tile several small detectors for use in a slot-system.

The large number of detector elements required for the slot-detector requires the use of a read-out technique that is fast and accurate. A CCD is particularly well suited to this application. As CZT is a relatively new material, the technology required to make a CCD directly on CZT as a monolithic device is not available. Instead, the read-out device is constructed of silicon and the CZT is indium-bump bonded to it, to provide the electronic connection to each detector element in the CZT photoconductor array. A simplified cross-section of this device is shown in Figure 1.

One difficulty in using CZT is due to its relatively low hole mobility[5]. Holes can only move a short distance in CZT before becoming trapped, causing loss of signal. This leads to gain variations and possibly poor temporal response. To minimize the influence of poor hole mobility, the CZT should be as thin as possible, and biased correctly to provide the shortest distance for the holes to travel.

Using the physical properties of CZT, the characteristics of the scanning technique and present limitations in CZT fabrication, careful modeling of the signal and noise propagation through the scanning system can be performed. From this model, important design parameters affecting image quality can be identified.

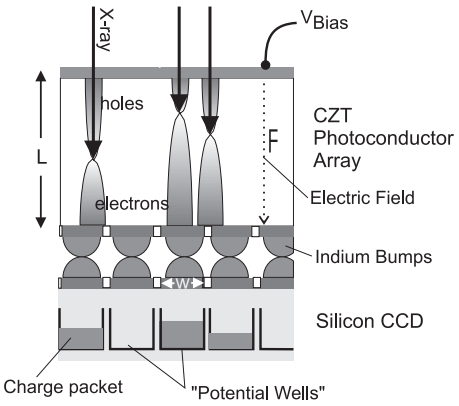

Figure 1. Schematic of a CZT photoconductor array bonded to a silicon CCD.

4. Image Quality Model

To determine the design criteria for the prototype detector, an image quality model was used. This model is based on a cascaded linear systems analysis, examining signal and noise propagation through various stages. These stages can be categorized as one of four mechanisms: gain, blurring, noise addition, and aliasing. In depth discussion of these mechanisms is described elsewhere [6, 7, 8]. Once the signal and noise equations have been calculated, the detective quantum efficiency (DQE) as a function of spatial frequency, f, can be calculated as follows:

$$DQE(f) = \frac{SNR^2_{out}(f)}{SNR^2_{in}(f)} \quad (1)$$

$$= \frac{k^2 \phi MTF^2(f)}{NPS(f)} \quad (2)$$

where k is the scaling factor for the detector, ϕ is the incident x-ray fluence, $MTF(f)$ is the modulation transfer function, and $NPS(f)$ is the noise power spectrum. The cascaded linear-systems analysis provides a powerful means of predicting the DQE(f) as well as determining critical stages and parameters that limit image quality.

4.1. INTERACTION STAGES

The CZT-based scanning system has been modeled as a set of nine stages, and the analysis as been performed in both the slot (along the axis of the detector) and scan directions. The stages are shown in Figure 2. The relevant design parameters are listed in Table 1. The most important stages, with respect to resolution loss, and image quality limitations are described in the following sections.

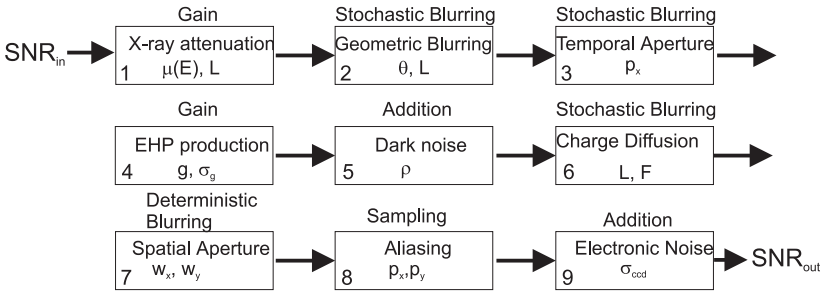

Figure 2. The nine stages of signal and noise propagation for the image quality model of the CZT-based detector.

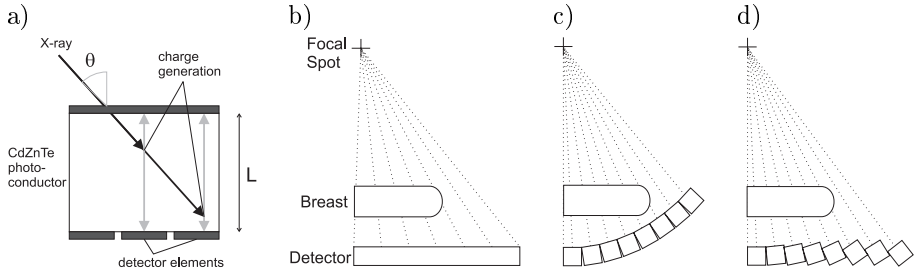

Figure 3. Geometric blurring is shown in a). This effect is strong in the planar geometry shown in a), because of the large incidence angle at the edge of the detector. Using a piece-wise curved geometry, the incidence angle is reduced as shown in b) and c).

4.1.1. *Geometric Blurring*

Because of the fan beam geometry of the x-ray field, the x-rays will be obliquely incident on the detector. As shown in Figure 3a, the x-ray can be absorbed anywhere along the path defined by the incidence angle, θ. This leads to a blur in the image of the form[9]:

$$MTF_{geo}(f_y) = \sqrt{\frac{\left(1 - e^{-\frac{\mu L}{\cos\theta}}\right)^2 + 4e^{-\frac{\mu L}{\cos\theta}} \sin^2(\pi f_y L \tan\theta)}{(1 - e^{-\mu\frac{L}{\cos\theta}})\left[1 + (2\pi f_y \frac{\sin\theta}{\mu})^2\right]}} \tag{3}$$

where f_y is the spatial frequency in the long axis of the detector (slot direction), L is the thickness of the detector, and μ is the linear attenuation coefficient. If a planar detector geometry is used as shown in Figure 3b, with a 60 cm source-detector distance and a 24 cm slot length, then the maximum incidence angle will be 22°. To reduce this effect, the detector can be designed as a piece-wise curved unit as shown in Figure 3c-d. If 2 cm detector elements are used, this reduces the incidence angle to 1.9°.

4.1.2. *Temporal Aperture Blurring*
During TDI acquisition, the charge signal is transferred from row to row at discrete clock intervals. Between transfers, however, the detector is moving, so that a detector element sweeps out a distance greater than its physical size. This additional distance is equal to the detector element pitch in the scan direction, p_x, before charge transfer. This causes an additional blurring in the scan direction.

$$MTF_{scan}(f_x) = \mathrm{sinc}(p_x f_x) \tag{4}$$

Note that this blurring is not the physical aperture blurring defined by the electrode (see below).

4.1.3. *Charge Diffusion*
Under the influence of the applied electric field, the electrons and holes are swept to opposite surfaces of the detector. During the time it takes for the charge carriers to move through the detector, the carriers can migrate laterally by diffusion. Que and Rowlands[9] have derived the MTF describing blur induced by this diffusion:

$$MTF_{diff}(f) = \frac{\mu\left(e^{-4kT\pi^2 f^2 L/(qF)} - e^{-\mu L}\right)}{\left[\mu - 4kT\pi^2 f^2/(qF)\right]\left(1 - e^{-\mu L}\right)} \tag{5}$$

where k is Boltzmann's constant, T is the temperature, L is the thickness of the semiconductor, F is the electric field in the semiconductor, and q is the elementary charge.

4.1.4. *Aperture Blurring*
In a digital detector, the resolution is primarily defined by the sensitive detector element area, or aperture. If the sensitive width is w_x, then the aperture blurring is:

$$MTF_{ap}(f_x) = \mathrm{sinc}(w_x f_x) \tag{6}$$

A similar equation can be used to define the aperture resolution in the y-direction (slot direction). If there is no "dead" space between each detector element then the sensitive width is equal to the pitch ($w_x = p_x,\ w_y = p_y$).

4.1.5. *Sampling*
Because the detector is divided into discrete elements, the detection method becomes a sampling operation. The sampling frequency is determined by the detector element pitch. One consequence of sampling is aliasing, in which high spatial frequency information is reflected down into lower frequencies. Aliasing violates the linear systems model. Cunningham[10] and Zhao[8] have shown that with certain assumptions, a reasonable pseudo-linear approach can be used. The first assumption is that the spatial frequency spectrum representing the object being imaged is band-limited to the Nyquist frequency, such that no aliasing of the signal is produced. Without aliasing, the MTF after sampling is simply the pre-sampling MTF, limited to the spatial frequencies below Nyquist. Unfortunately, the high spatial frequency noise cannot be dismissed with the same assumption, and as a result, the NPS after aliasing takes the form:

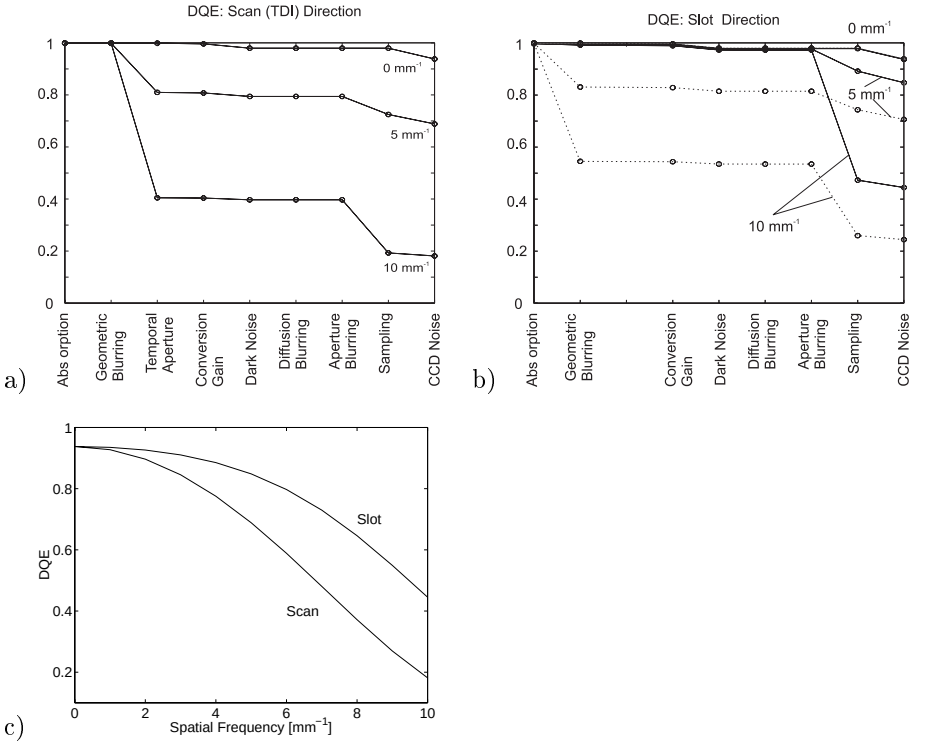

Figure 4. DQE as a function of stage in the a) scan and b) slot directions. The DQE is shown at 0, 5 and 10 mm^{-1}. The total system DQE is shown in c).

$$NPS_{alias}(f) = \sum_{i=-\infty}^{\infty} NPS(f + i \cdot F_{Ny}) \tag{7}$$

where F_{Ny} is the Nyquist frequency. This increase in low spatial frequency noise causes a corresponding decrease in DQE(f).

It should be noted that this approach to the linearization of the sampling stage may not be completely satisfactory[11], and a more rigorous model may be required.

5. Results

The model outlined above was used to calculate the DQE for the design parameters listed in Table 1. Figure 4 shows the DQE(f) as a function of stage at 0, 5 and 10 mm^{-1} for the slot and scan direction. Clearly the most important sources of image degradation are temporal aperture blurring and aliasing due to sampling. Geometric blurring would also be a factor if a planar geometry were used, as shown by the dotted lines in Figure 4b.

As the model parameters can be varied easily, this can be incorporated into a powerful tool to predict the best parameters for optimum image quality. For

pitch (p_x, p_y)	50 μm	x-ray energy (E)	20 keV
active width (w_x, w_y)	50 μm	exposure (X)	0.001 R
thickness (L)	0.5 mm	incidence angle (θ)	2° or 12°
resistivity (ρ)	5 GΩ	electronic noise (σ_{CCD})	1000 e^- / pixel
electric field (F)	0.5 V/μm		

TABLE 1. Parameters used for calculation of the DQE in Figure 4

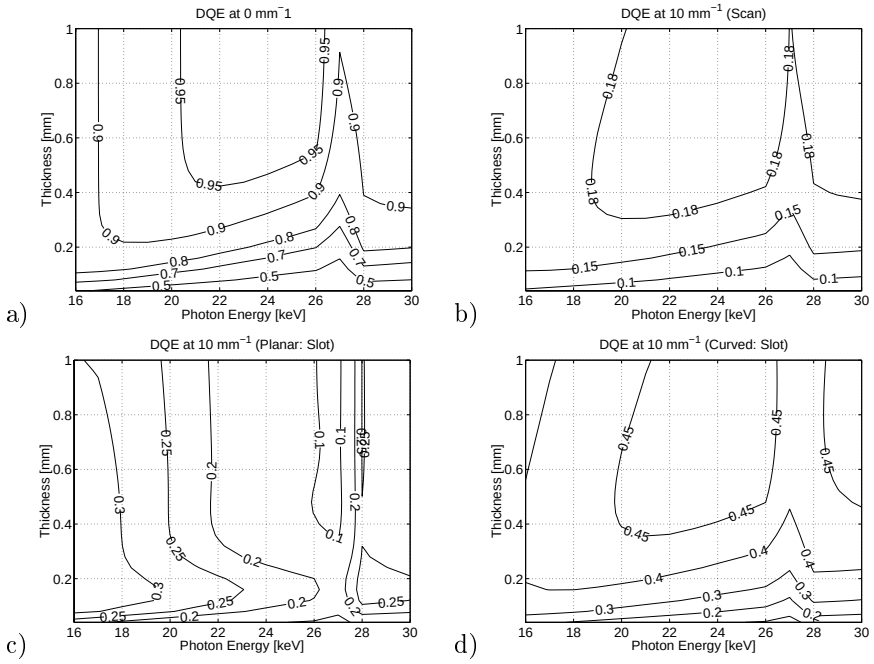

Figure 5. Contour plot of DQE as a function of CZT thickness and photon energy. Shown is a) the DQE at 0 mm^{-1}, b) at 10 mm^{-1} for the scan direction, and at 10 mm^{-1} for the slot directions in a c) planar and d) curved geometry.

example, the thickness and photon energy can be varied over a range (0 - 1 mm, and 16 to 30 keV), with all other parameters were held fixed (Table 1). The results are shown in the contour plots in Figure 5 for zero spatial frequency DQE, and the DQE at 10 mm^{-1} for the slot and scan directions in both the planar and curved geometries described in the previous section.

For the planar geometry (Figure 5c), there is a clear optimum thickness at 0.15 mm, at which the DQE(f) is highest over the greatest energy range. Although using thicker CZT improves quantum efficiency, the loss in DQE(f) due to the geometric effect counter-acts this improvement. Using curved geometry, this limitation is removed and the DQE(f) tends to improve with thickness (up to 0.5 mm).

6. Discussion

Future work will involve the improvement and verification of the detector model. One important phenomenon that will need to be incorporated is incomplete charge collection due to hole trapping and recombination[12]. This effect causes a significant increase in gain variation at the conversion stage and it may cause a temporal lag that introduces blurring in the scan direction, similar to that seen in other imaging devices[8, 13]. However, because of the "small pixel" geometry, gain variations due to hole trapping are greatly reduced[14]. As a result, incorporation of hole trapping into the model should be a small correction.

7. Summary

We are developing a direct conversion detector for a slot-scanned digital mammography system. To help in the design, a model has been developed that will predict image quality. From the model, the primary stages involved in image quality degradation are geometric blurring, temporal aperture blurring due to the TDI acquisition technique, and aliasing. This model can be used to optimize the design to provide the best possible image quality, given the limitations of the detector technology, and the requirements of the imaging task for mammography.

References

[1] Barber HB, Barrett HH, Augustine FL, Hamilton WJ, Apotovsky BA, Dereniak EL, Doty FP, Eskin JD, Garcia DG, Matherson KJ, Woolfenden JM, and Young ET. Development of a 64 x 64 CdZnTe array and associated integrated circuit for use in nuclear medicine. J. of Elect. Mat. 26, 765–772 (1997).

[2] Yaffe MJ. Digital mammography. In Haus AG and Yaffe MJ(eds.), *Syllabus: A Categorical Course in Physics Technical Aspects of Breast Imaging*. RSNA, Oak Brook, IL, 1993, pp. 271–282.

[3] Karssemeijer A, Frieling J, and Hendriks JHCL. Spatial resolution in digital mammography. Invest. Radiol. 28, 413–419 (1993).

[4] Fahrig R and Yaffe MJ. Optimization of spectral shape in digital mammography. Medical Physics 21, 1473–1481 (1994).

[5] Barber HB. Application of II-VI materials to nuclear medicine. J. of Elect. Mat. 25, 1232–1238 (1996).

[6] Cunningham IA. Analyzing system performance. In Frey GD and Sprawls P(eds.), *The Expanding Role of Medical Physics in Diagnostic Imaging*. AAPM, 1997, pp. 231–263.

[7] Henry J, Yaffe MJ, and Tumer TO. Noise in hybrid photodiode array - ccd x-ray image detectors for digital mammography. Proc. SPIE 2708, 106–115 (1996).

[8] Zhao W and Rowlands JA. Digital radiology using active matrix readout of a-Se: Theoretical analysis of detective quantum efficiency. Med. Phys. 24, 1819–1833 (1997).

[9] Que W and Rowlands JA. X-ray imaging using amorphous selenium: inherent spatial resolution. Medical Physics 22, 365–374 (1995).

[10] Cunningham IA. Degradation of the detective quantum efficiency due to a non-unity fill factor. Proc SPIE 3032, 22–31 (1997).

[11] Dobbins III JT. Effects of undersampling on the proper interpretation of MTF, NPS, and NEQ of digital imaging systems. Medical Physics 22, 171–181 (1995).

[12] Nemirovksy Y, Ruzin A, Asa G, and Gorelik J. Study of the charge collection efficiency of CdZnTe radiation detectors. J. of Elect. Mat. 25, 1221–1231 (1996).

[13] Mainprize JG. Effect of phosphor persistence on image quality in digital x-ray scanning systems. Proc. SPIE 2708, 85–94 (1996).

[14] Eskin JD, Barrett HH, Barber HB, and Woolfenden JM. The effect of pixel geometry on spatial and spectral resolution in a CdZnTe imaging array. In Moonier PA(ed), *IEEE Nuclear Science Symposium and Medical Imaging Conference Record*, volume 1, pp. 544–468, 1995.